THE JOURNAL OF PHYSICAL CHEMISTRY B

Article

pubs.acs.org/JPCB

Utilizing Afterglow Magnetization from Cross-Polarization Magic-Angle-Spinning Solid-State NMR Spectroscopy to Obtain Simultaneous Heteronuclear Multidimensional Spectra

James R. Banigan and Nathaniel J. Traaseth*

Department of Chemistry, New York University, New York, New York 10003, United States

ABSTRACT: The time required for data acquisition and subsequent spectral assignment are limiting factors for determining biomolecular structure and dynamics using solid-state NMR spectroscopy. While strong magnetic dipolar couplings give rise to relatively broad spectra lines, the couplings also mediate the coherent magnetization transfer via the Hartmann−Hahn cross-polarization (HH−CP) experiment. This mechanism is used in nearly all backbone assignment experiments for carrying out polarization transfer between ^{1}H, ^{15}N, and ^{13}C. In this Article, we describe a general spectroscopic approach to use the residual or "afterglow" magnetization from the ^{15}N to ^{13}C selective HH−CP experiment to collect a second multidimensional heteronuclear data set. This approach allowed for the collection of two commonly used sequential assignment experiments (2D NCA and NCO or 3D NCACX and NCOCX) at the same time. Our "afterglow" technique was demonstrated with uniformly [^{13}C,^{15}N] and [1,3-^{13}C] glycerol-labeled ubiquitin using instrumentation available on all standard solid-state NMR spectrometers configured for magic-angle-spinning. This method is compatible with several other sensitivity enhancement experiments and can be used as an isotopic filtering tool to reduce the spectral complexity and decrease the time needed for assignment.

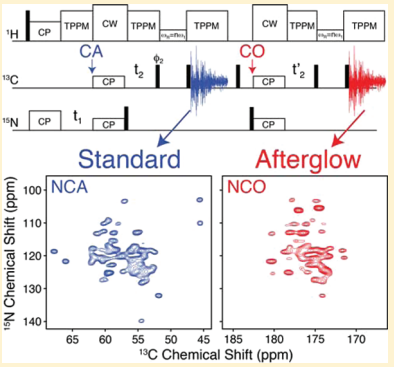

INTRODUCTION

Solid-state NMR magic-angle-spinning (SSNMR MAS) is a widely employed method to probe structure and dynamics of hard and soft matter.[1−7] One of the main bottlenecks is biomolecular spectral assignment, which can be especially challenging for membrane proteins and amyloid samples. To address this problem, a number of ways have been proposed to improve the spectral resolution and sensitivity of data acquisition. These can be broadly grouped into three categories: (1) spectroscopic-based (e.g., pulse sequences, data acquisition), (2) sample preparation (e.g., isotopic labeling, paramagnetic labeling), and (3) advances in instrumentation (e.g., multiple receivers, cryogenic probes). Combined spectroscopic and instrumentation approaches such as simultaneous or sequential data acquisitions have been applied to the time-consuming process of spectral assignment through the improvement of triple resonance techniques that shorten data acquisition times.[8−11]

A novel solution NMR approach recently introduced by Kupce et al. utilizes the residual or "afterglow" ^{13}C magnetization for the purpose of acquiring multiple heteronuclear spectra at the same time.[9] In this pulse sequence, the ^{13}C magnetization was directly detected to acquire a 2D (HA)-CACO experiment on nuclease A inhibitor in the *standard* way. The residual ^{13}CO magnetization was then transferred to ^{15}N and finally detected using the sensitive $^{1}H_N$ magnetization in a 3D (HA)CA(CO)NNH experiment. Since ^{13}C and ^{1}H signals were detected, these experiments made use of parallel acquisition requiring two receivers. Unlike this solution NMR methodology that relied on *J*-couplings, the most important transfer mechanism in oriented and MAS SSNMR is the Hartmann−Hahn cross-polarization (HH−CP).[12−15] This experiment uses matched spinlocks on two channels, resulting in coherent polarization transfer from one nucleus to the other. Since the CP is the basic element for nearly all SSNMR applications, a tremendous amount of effort has been devoted to understanding and improving this experiment,[16−20] including the use of multiple contact pulses.[12,21] For protein applications, transfer of magnetization among low frequency ^{15}N and ^{13}C nuclei most commonly utilizes the double CP experiment[22−26] or other novel polarization transfer approaches.[27−32]

An application of the CP experiment was recently demonstrated using RNA in SSNMR spectroscopy. This triple resonance cross-polarization method uses ^{1}H to simultaneously polarize ^{13}C and ^{15}N with subsequent parallel acquisition using two receivers.[8] This scheme has been further advanced to obtain sequentially acquired data sets that give homonuclear and heteronuclear ^{13}C−^{15}N correlation spectra using a single receiver (DUMAS).[10,72] Careful optimization of the simultaneous cross-polarization will give only small losses on the transfer from ^{1}H to both ^{15}N and ^{13}C as compared to the double resonance HH-CP experiment. These methods and others rely on relatively long ^{15}N and ^{13}C T_1 and $T_{1\rho}$ values in

Received: April 5, 2012
Revised: May 14, 2012
Published: May 14, 2012

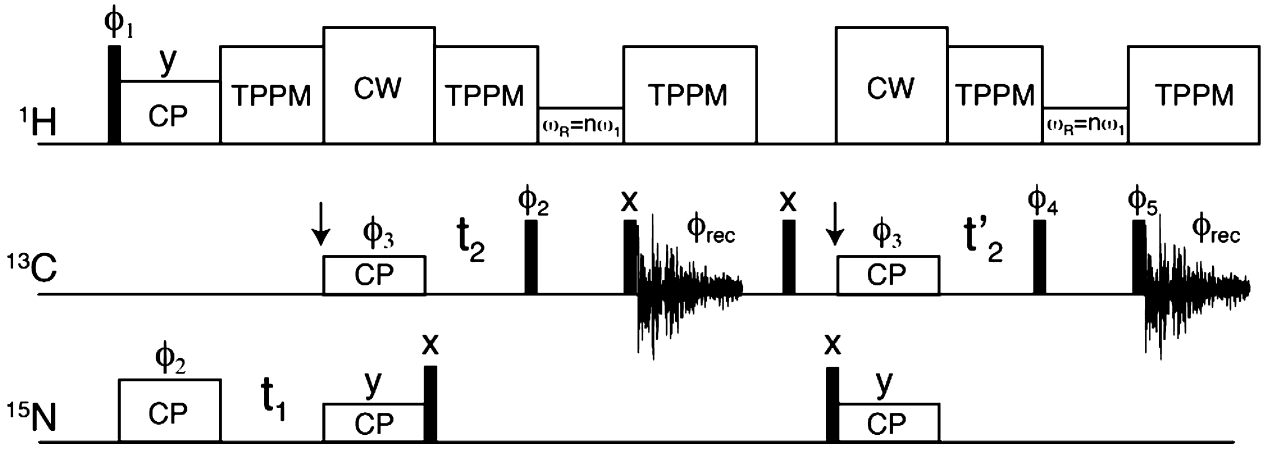

Figure 1. "Afterglow" pulse sequence with two acquisitions for simultaneous detection of 2D SIM_1-NCA and SIM_2-NCO or 3D SIM_1-NCACX and SIM_2-NCOCX spectra. The former are achieved by setting the DARR mixing time to zero. The DARR mixing can be replaced with a double quantum transfer for improved single bond transfers. The narrow rectangles correspond to 90° pulses. The left and right arrows within the ^{13}C channel signify the offset positioned on the ^{13}CA (57.5 ppm) and ^{13}CO regions (175 ppm), respectively. Phase are: $\phi_1 = (x,-x)$, $\phi_2 = (y)$, $\phi_3 = (x,x,y,y)$, $\phi_4 = (-y,-y,-x,-x)$, $\phi_5 = (y,y,-x,-x)$, and $\phi_{rec} = (x,-x,-y,y)$. To obtain phase-sensitive data in t_1 and t_2, ϕ_2 and ϕ_3 were phase-shifted by 90°, respectively. After the first FID acquisition, a 5 ms time was allowed to dephase residual ^{13}C. The pulse sequence in Figure 1 can be downloaded from our Web site: www.nyu.edu/fas/dept/chemistry/traasethgroup/.

soft matter, including membrane proteins in oriented lipid bilayers.[33,34]

To improve the efficiency of data acquisition in SSNMR MAS, we describe an approach to detect residual or "afterglow" magnetization resulting from the double CP experiment involving selective transfer from ^{15}N to ^{13}CA. We show that this ^{15}N magnetization is appreciable and can be used to obtain a second multidimensional heteronuclear correlation experiment with good sensitivity. In practice, the result is the detection of two 2D (NCA and NCO) or two 3D (NCACX and NCOCX) experiments at the *same time* (i.e., *two for the price of one*). These experiments do not require special instrumentation and, therefore, are applicable to all spectroscopic approaches where residual coherence can be salvaged for increasing the speed of data acquisition.

EXPERIMENTAL METHODS

Sample Preparation. Ubiquitin was expressed in BL21-(DE3) *E. coli* bacteria in the presence of uniformly labeled $^{13}C_6$-glucose and ^{15}N-ammonium chloride in minimal media (M9) and purified as previously described.[35] The glycerol labeling experiment was achieved by replacing glucose with [1,3-^{13}C] glycerol (1 g/L) and natural abundance sodium carbonate (1 g/L).[36,37] For preparation of the solid-state NMR samples, 10 mg of ubiquitin was dissolved in 400 μL of 20 mM sodium citrate at pH 4.1. Crystallization was initiated by the dropwise addition of 2-methyl-2,4-pentanediol (MPD) to a final concentration of 60% and allowed to incubate overnight at 4 °C.[38] The samples were packed into 3.2 mm MAS rotors using sample spacers to prevent sample dehydration.

NMR Spectroscopy. All NMR experiments were carried out using a DDR2 Agilent NMR spectrometer operating at a ^1H frequency of 600 MHz. The temperature was set to 0 °C, and the MAS rate was 12 500 ± 5 Hz. The initial cross-polarization contact time from ^1H to ^{15}N was set to 1 ms. The transfers between ^{15}N to ^{13}CA and ^{15}N to ^{13}CO utilized SPECIFIC−CP,[23] a form of double CP,[25] where the ^{15}N offset was set to 121 ppm, the ^{13}CA offset to 57.5 ppm, and the ^{13}CO offset to 175 ppm. The ^{15}N to ^{13}CA transfer used a tangent adiabatic ramp[22] on the ^{13}C channel, while the ^{13}CO SPECIFIC−CP utilized the ramp on the ^{15}N channel. The $\Delta/2\pi$ and $\beta/2\pi$ parameters of the adiabatic cross-polarization were set to 1.2 and 0.3 kHz for the ^{15}N to ^{13}CA transfer and 3.7 and 0.9 kHz for the ^{15}N to ^{13}CO transfer (see eqs 1 and 2 of Franks et al.[39]) with the total time of the cross-polarization set to 4 ms. All parameters were optimized to obtain maximal signal intensity in the standard 1D NCO and NCA experiments. Both sequential data acquisition periods used a ^{13}C spectral width of 100 kHz and an acquisition time of 20 ms. The indirect ^{15}N dimension was acquired with a spectral width of 3125 Hz and 28 increments. A total of 64 and 128 scans were used for the [U−^{13}C,^{15}N] and [1,3-^{13}C] glycerol-labeled ubiquitin samples, respectively. For spin diffusion experiments, the DARR condition was set to the $n = 1$ rotary resonance condition on ^1H (12.5 kHz).[40]

RESULTS

Sequential Acquisition of Afterglow ^{15}N Magnetization. The standard experiments for obtaining resonance assignments and distance restraints in MAS utilize multiple transfers between ^{15}N and ^{13}CA or ^{15}N and ^{13}CO. The NCACX and NCOCX experiments are two of the most valuable that give correlations among the backbone nuclei. The former correlates ^{13}C with the chemical shifts of ^{15}N and ^{13}CA. This involves a HH−CP element where ^1H polarization is transferred to ^{15}N and followed by a ^{15}N chemical shift evolution in t_1. Magnetization is then most commonly transferred to ^{13}CA using a type of double cross-polarization[25] called SPECIFIC−CP.[23] After the transfer, ^{13}CA chemical shifts are evolved in the t_2 time dimension and then allowed to undergo spin diffusion typically with a DARR mixing period.[40] Finally, the ^{13}C magnetization is detected in the direct dimension. These are the standard experiments carried out and will be referred to as the STD-NCA or STD-NCACX (with DARR).

Following the SPECIFIC−CP transfer to ^{13}CA, there is residual ^{15}N magnetization remaining that is typically discarded. Using [U−^{15}N,^{13}C] ubiquitin, we carried out the 1D STD-

NCA experiment detecting on ^{15}N immediately following the SPECIFIC−CP transfer to ^{13}CA. Relative to the starting ^{15}N magnetization, ∼40−45% of the ^{15}N signal remained. Therefore, it is possible to detect this ^{15}N polarization at the same time as the STD-NCA ^{13}C detected experiment with a second receiver (parallel acquisition[11]). However, 1D spectra do not provide the resolution required for adequately observing the protein resonances. Instead, the pulse sequence in Figure 1 shows how an "afterglow" (or residual) ^{15}N signal can be salvaged to obtain a second 2D NCO or 3D NCOCX data set. The first half of the pulse sequence in Figure 1 is identical to that of a STD-NCA (or STD-NCACX) experiment. To reuse the residual ^{15}N magnetization, a 90° pulse is applied to ^{15}N spins immediately following the SPECIFIC−CP transfer to ^{13}CA. This stores the magnetization along the z-axis. Since the T_1 relaxation times for ^{15}N in proteins are on the order of seconds, placing the spins along the z-axis results in only a small amount of magnetization lost due to longitudinal relaxation. Following the free-induction-decay acquisition for the 2D NCA (or 3D NCACX) experiment, a 90_x° pulse is applied to ^{15}N, placing it along the y-axis. Next, a second SPECIFIC−CP step is used to transfer magnetization to ^{13}CO in the same way as a standard NCO experiment. The ^{13}CO magnetization is then directly detected to obtain a 2D NCO or evolved in the indirect t_2' dimension followed by a DARR mixing element to give a 3D NCOCX experiment. If evolved in the indirect dimension, t_2' is arrayed concurrently with the ^{13}CA t_2 period for the NCACX experiment. Both simultaneously acquired data sets have an identical ^{15}N chemical shift evolution period (t_1). For brevity, we will refer to the sequentially acquired data sets using the following nomenclature: SIM$_1$-NCA or SIM$_1$-NCACX (first data set acquired) and SIM$_2$-NCO or SIM$_2$-NCOCX (second data set acquired); the standard experiments will be called STD-NCA, STD-NCO, STD-NCACX, or STD-NCOCX.

Application to Uniformly Labeled Ubiquitin. We carried out the pulse sequence in Figure 1 on selectively and uniformly labeled ubiquitin prepared in a microcrystalline state. [U−^{13}C,^{15}N] ubiquitin has 76 residues and therefore 76 ^{15}N−^{13}CA pairs. The 2D STD-NCA and SIM$_1$-NCA data sets on [U−^{13}C,^{15}N] ubiquitin are shown in Figure 2. These spectra give the same signal/noise, which is expected since the first half of the pulse sequence in Figure 1 is identical to the STD-NCA experiment. After the first transfer from ^{15}N to ^{13}CA, the amount of ^{15}N magnetization available for the ^{15}N to ^{13}CO SPECIFIC−CP is reduced. This results in an overall signal intensity of the SIM$_2$-NCO 2D data set of 32 ± 3% compared to that of the STD-NCO. However, the SIM$_2$-NCO gives ∼50% of the signal/noise as the SIM$_1$-NCA, which results from the slightly better efficiency of the ^{15}N to ^{13}CO vs ^{15}N to ^{13}CA SPECIFIC−CP experiment.[39,41] Although the second data set is lower in intensity (see 1D cross sections in Figure 3), the SIM$_2$-NCO is a *free* data set since the preparation and subsequent detection of the "afterglow" ^{15}N magnetization only adds ∼25 ms to the overall pulse sequence. In practice, for a recycle delay of 2 s and an acquisition period of 25 ms, the pulse sequence in Figure 1 only increases the experimental time by 1.2% relative to the STD-NCA.

There are ∼45−50 resonances within each of the NCA spectra shown in Figure 2. It has been reported that nine peaks do not appear as a result of residual motion in the loop encompassing residues 8−10 and the C-terminus (residues 71−76) at 0 °C.[38] In addition, some of the peaks have reduced signal intensity based on crystallization with MPD or

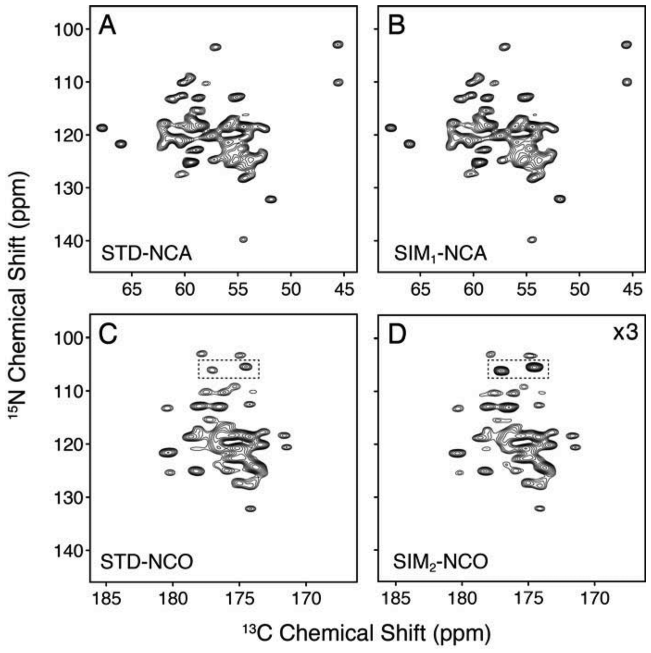

Figure 2. Comparison of the standard vs sequentially acquired data sets on [U−^{13}C,^{15}N] ubiquitin. The STD-NCA and STD-NCO data sets (A and C) used experimental parameters identical to the sequentially acquired ones (B and D). The spectra in panels A and B are each plotted starting at a contour level of 18.75. This is a factor of 1.5 higher than the SIM$_2$-NCO data set (panel D; first contour: 12.5). The SIM$_2$-NCO spectrum (panel C) is plotted at 3 times the signal level compared to the STD-NCO (first contour: 37.5), which accounts for the signal loss in the SIM$_2$-NCO from the SPECIFIC−CP transfer to ^{13}CA. For the listed contour levels, the standard deviation of the noise is 1.0. The peaks in the dotted rectangles indicate side chain residues that have 75% intensity retention in panel D relative to panel C. The 2D data sets for the STD-NCA and STD-NCO required 2 times longer acquisition than that for the SIM$_1$-NCA and SIM$_2$-NCO.

polyethylene glycol (PEG).[42] For example, in the 2D NCA spectrum reported by Seidel et al. crystallized from PEG, there are four clearly resolved Gly peaks (G10, G35, G47, and G53); however, in the ubiquitin N-CA spectrum reported by Schubert et al. prepared by crystallization using MPD (same as the ubiquitin preparations used in this study), only G35 and G47 were observed.[43] The lack of the Gly10 peak is consistent with the cross-polarization-based results from Igumenova et al.[38] These observations from the literature as well as our detection of an additional ∼3−5 peaks at a reduced contour level from the data in Figure 2 account for the large majority of the expected resonances in ubiquitin. To identify the remaining spin systems, experiments at a higher magnetic field and/or 3D spectroscopy can be used.[44]

The 3D version of the SIM$_2$-NCOCX and SIM$_1$-NCACX data sets evolve the ^{13}CO and ^{13}CA dimensions together in t_2' and t_2, respectively. It is important to realize that the dwell times for the ^{13}CO and ^{13}CA dimensions can be different, which is beneficial since the ^{13}CA chemical shift range is ∼30 ppm, while the ^{13}CO region is ∼10 ppm (a factor of 3). Therefore, it is possible to reduce the number of increments in the indirect ^{13}CO dimension by a factor of 3 and increase the number of scans by the same factor to obtain identical acquisition times in t_2 and t_2'. Alternatively, one may acquire additional indirect points in t_2 or t_2'.[10] For example, ^{13}CO nuclei typically have a longer T_2 relaxation time in proteins

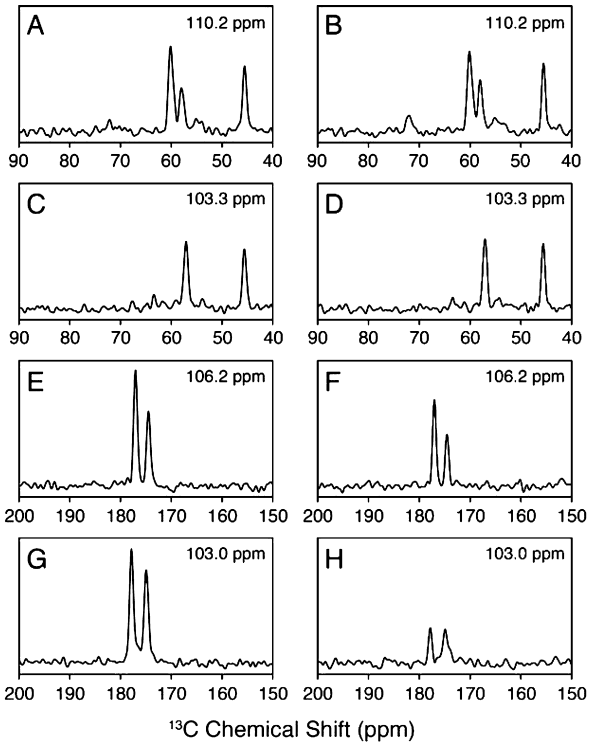

Figure 3. 1D cross sections of the 2D spectra shown in Figure 2 for [U−^{13}C,^{15}N] ubiquitin. The ^{15}N frequencies are given in each panel. The STD-NCA 1D cross sections (A, C) can be directly compared with those of the SIM$_1$-NCA data set (B, D). As expected, these peak intensities are identical. The STD-NCO cross sections (E, G) are directly compared to those of the SIM$_2$-NCO (F, H). The noise level is the same in all 1D spectra. The spectra in panels E and F correspond to side chain ^{15}NH$_2$ resonances.

relative to ^{13}CA, allowing for increased sampling of the maximum t_2' in the SIM$_2$-NCOCX experiment, which would increase the resolution. These linear correction factors have previously been described in the DUMAS technique.[10]

It should also be stated that while the first DARR mixing time is intended for only the ^{13}C spins, the ^{15}N magnetization stored along the *z*-axis may also undergo spin diffusion. However, this will be relatively minor (<5%) for typical mixing times of ∼200 ms.[42] It is also noted that the order of the sequentially acquired experiments can be inverted to detect the NCO first (i.e., SIM$_1$-NCO), followed by the SIM$_2$-NCA experiment. In this case, the SIM$_1$-NCO will give the same signal/noise as the STD-NCO, while the SIM$_2$-NCA spectrum will have ∼33% of the signal/noise as the STD-NCA experiment.

Distinguishing Side Chain NH$_2$ Peaks in the Spectrum. In the SIM$_2$-NCO spectrum, it was also possible to easily distinguish the side chain NH$_2$ peaks from those of backbone amides in [U−^{13}C,^{15}N] samples. For side chain Asn or Gln residues, the ^{15}N to ^{13}CA SPECIFIC−CP did not transfer amine ^{15}N magnetization to ^{13}C spins since the covalent C_γ (Asn) or C_δ (Gln) nuclei have chemical shifts of ∼175 ppm (^{13}CA offset for the experiment was ∼57.5 ppm). Therefore, only a small loss in side chain signal (∼25%) was observed in the SIM$_2$-NCO spectrum relative to that of the STD-NCO. The side chain amine peaks are highlighted in the SIM$_2$-NCO experiment in Figure 2 and displayed as 1D cross sections in Figure 3E and F. For [U−^{13}C,^{15}N] samples, this means these peaks are the most intense in the spectrum and are easily distinguishable from those of the backbone NCO cross-peaks. Since the ^{15}N amine resonances can overlap with those from the amide ^{15}N of Ser, Gly, and Thr, the intensity of the peaks can be used to easily distinguish these residue types for the purpose of spectral assignment.

Application to Selective Glycerol Labeling in Ubiquitin. A common way to improve resolution and reduce spectral congestion is the use of selective labeling schemes.[45,46] One of the preferred methods is glycerol labeling ([1,3-^{13}C] or [2-^{13}C]) that significantly reduces pairwise ^{13}C labels (i.e., few ^{13}C−^{13}C covalent bonds). This decreases resonance linewidths by removing one-bond ^{13}C−^{13}C *J*-couplings and eliminates many of the resonances in a given spectrum.[36,37] It is also common to use glycerol or reverse labeling[47] in conjunction with double CP[48,49] or REDOR-based dephasing[50−53] to assist in the assignment process.[48,49] We applied our "afterglow" pulse sequence to ubiquitin labeled with [1,3-^{13}C] glycerol and detected SIM$_1$-NCA and SIM$_2$-NCO 2D spectra at the same time (Figure 4). Selected 1D cross sections of the 2D spectra are also shown in Figure 5. As expected from the isotopic labeling pattern, we found that several peaks in the NCA- and NCO-based spectra were absent (e.g., Gly resonances at 45 ppm in the SIM$_1$-NCA).[36,37] On average we observed that the SIM$_2$-NCO gave 63 ± 9% of the sensitivity compared to the

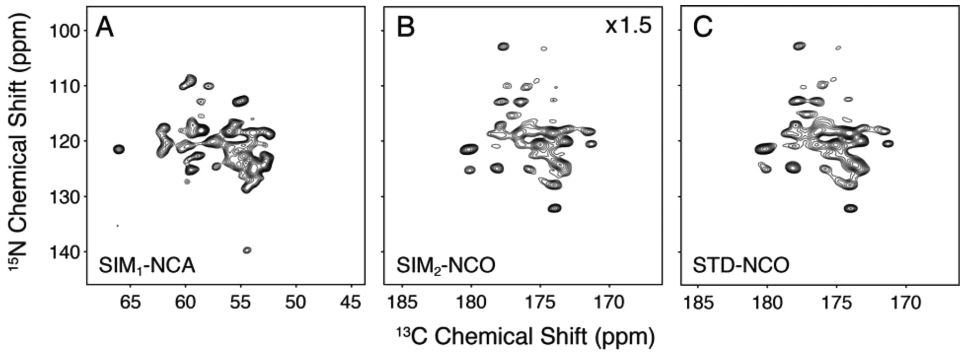

Figure 4. Comparison of the standard vs sequentially acquired data sets on [1,3-^{13}C] glycerol labeled ubiquitin. The STD-NCA (not shown) is identical to that of the SIM$_1$-NCA (panel A). All comparable experimental parameters were the same between the STD-NCO (panel C) and the SIM$_2$-NCO (panel B). The sequentially acquired data sets in panels A and B are plotted at the same noise level (first contour: 11.0). The SIM$_2$-NCO spectrum (panel B) is plotted at 1.5 times the signal level compared to the STD-NCO (panel C; first contour: 16.5); this accounts for the average signal loss in the SIM$_2$-NCO due to the SPECIFIC−CP transfer to ^{13}CA. For the listed contour levels, the standard deviation of the noise is 1.0.

dx.doi.org/10.1021/jp303269m | *J. Phys. Chem. B* 2012, 116, 7138−7144

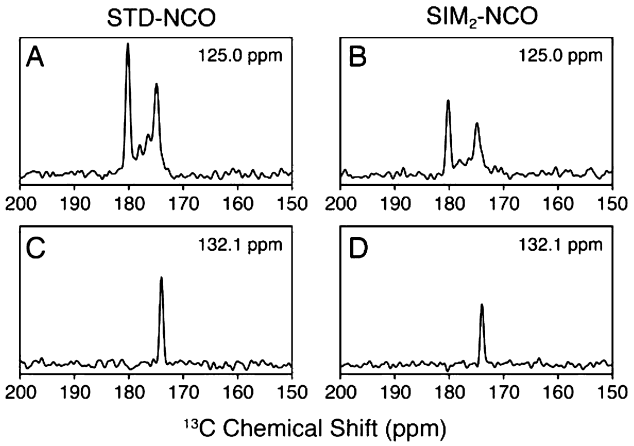

Figure 5. 1D cross sections of the 2D spectra shown in Figure 4 for the [1,3-^{13}C] glycerol-labeled ubiquitin sample. The ^{15}N frequencies indicated in each panel are directly comparable for the STD-NCO (A, C) and SIM$_2$-NCO spectra (B, D). The noise level is the same for the four 1D cross sections.

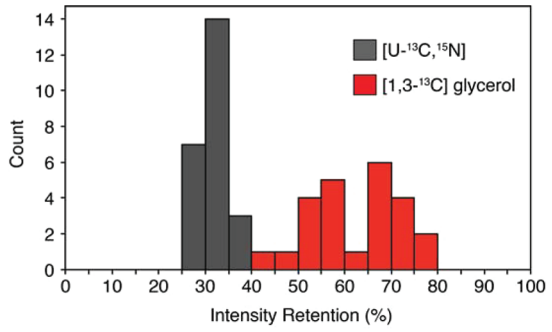

Figure 6. Histogram of intensity retentions for the [1,3-^{13}C] glycerol vs [U−^{13}C,^{15}N] labeling ubiquitin samples. The intensity retention is calculated by dividing the intensity of the resolved peak in the 2D SIM$_2$-NCO spectrum by the corresponding resonance in the 2D STD-NCO. In total, 24 resolved peaks from the 2D spectra from Figures 2 and 4 were used for this analysis. The average ± standard deviation for the two samples are: [U−^{13}C,^{15}N] = 32 ± 3% and [1,3-^{13}C] glycerol = 63 ± 9%.

STD-NCO spectrum (Figure 6). The primary advantage of our approach for partially labeled samples is to maintain no loss in sensitivity for the SIM$_1$-NCA data set while also obtaining a complementary data set compared to what would be obtained for [U−^{13}C,^{15}N] samples. In other words, the ^{15}N to ^{13}CA SPECIFIC−CP element acts as an isotope filter that can be used to assign peaks.[48] For uniformly labeled samples, the spectral information for backbone amide peaks between STD-NCO and SIM$_2$-NCO contains identical information since all sites have ^{13}C labeling. However, for the [1,3-^{13}C] glycerol sample, the incorporation at the ^{13}CA depends on the residue type.[36,37] As a way to illustrate this, we plot the intensity retention as a histogram in Figure 6 comparing the uniform vs glycerol labeling. The retention was calculated as the SIM$_2$-NCO peak intensity divided by the same resonance in the STD-NCO. Only resolved peaks were used in this calculation, and all resonances analyzed are the same for the glycerol and uniform labeling. The wide distribution of intensity retentions compared to that obtained for the [U−^{13}C,^{15}N] ubiquitin sample shows that the sequential-acquisition approach can be used to assign resonances in a similar way as has been previously reported.[48,54]

DISCUSSION

Developments in magnetic resonance spectroscopy aim to improve the rate of biomolecular structure and dynamics determination and the speed and quality of image acquisition. We introduced a simple approach to utilizing residual or "afterglow" magnetization from the ^{15}N double CP experiment to obtain a second multidimensional data set that can be used to assign biomolecules by SSNMR. In current practice, this residual magnetization is neither refocused nor directly detected. Since one of the most important factors determining experimental length is the recycle time (time needed to obtain equilibrium), methods such as RELOAD[55] and use of paramagnetic agents[56−58] strive to reduce or eliminate the need for long delays. Our method detects two heteronuclear correlation spectra (NCA and NCO) back-to-back with no recycle delay between acquisition periods. This means two data sets can be acquired for essentially the same amount of time as the standard acquisition that gives only a single data set. For [U−^{13}C,^{15}N] ubiquitin, we have shown that the SIM$_2$-NCO gives 32% of the sensitivity of the STD-NCO data set and 50% of the signal/noise as the SIM$_1$-NCA. This means that an additional data set with excellent signal/noise can be obtained with no loss in sensitivity compared to the standard experiment. Related methods have utilized multiple cross-polarization elements to improve sensitivity[59] or cross-depolarization filtering techniques.[60] Note that it is possible to perform dual-band selective ^{15}N to ^{13}C double CP transfers,[26] but this compromises the sensitivity of the NCA region by ∼30%.

Our sequential acquisition method is also amenable to selective glycerol or reverse labeling approaches. Since these samples have dilute ^{13}C spins, it is possible to obtain two data sets with nearly the same signal/noise without compromising the sensitivity of the spectrum acquired first. An application of our approach is the use of selectively labeled protein samples to aide in the assignment of overlapped spectra. This is important for poorly dispersed ^{15}N signals such as membrane proteins that often do not allow for robust assignments from triple resonance experiments.[52,61] While some well-ordered membrane proteins give excellent spectra,[62−64] several other membrane proteins have biologically relevant conformational disorder[65−69] that gives rise to broader spectral lines. Future developments such as TROSY-based methods may aide in reducing ^{15}N linewidths that are broadened from N−H motion on the nanosecond to microsecond time scale.[70]

In summary, the presented method uses "afterglow" ^{15}N magnetization remaining from the initial double CP step to obtain a second high-quality data set. The acquisition of these 2D or 3D spectra relies on long $T_{1\rho}$ and T_1 relaxation times that exist for ^{15}N in SSNMR.[71] Our approach is also compatible with several existing techniques, including the DUMAS method,[10,72] paramagnetic-based sensitivity enhancement methods,[56−58] dynamic nuclear polarization experiments,[73] applications utilizing time-resolved MAS techniques,[74−76] and oriented SSNMR. This method requires no additional SSNMR hardware and will result in no loss in sensitivity for the first data set. The second data set is *free* and can be detected with good sensitivity for biomolecular assignments in MAS SSNMR spectroscopy.

dx.doi.org/10.1021/jp303269m | J. Phys. Chem. B 2012, 116, 7138−7144

AUTHOR INFORMATION

Corresponding Author

*Phone: (212) 992-9784. E-mail: traaseth@nyu.edu.

Notes

The authors declare no competing financial interest.

ACKNOWLEDGMENTS

The authors thank Prof. Alexej Jerschow for a careful reading of the manuscript. This work was supported by NIH grant 5K22AI083745 and start-up funds from New York University.

REFERENCES

(1) McDermott, A. E. *Curr. Opin. Struct. Biol.* **2004**, *14*, 554−561.
(2) Opella, S. J.; Marassi, F. M. *Chem. Rev.* **2004**, *104*, 3587−3606.
(3) Hong, M. *J. Phys. Chem. B* **2007**, *111*, 10340−10351.
(4) Tycko, R. *Annu. Rev. Phys. Chem.* **2011**, *62*, 279−299.
(5) Baldus, M. *Curr. Opin. Struct. Biol.* **2006**, *16*, 618−623.
(6) Naito, A. *Solid State Nucl. Magn. Reson.* **2009**, *36*, 67−76.
(7) Wylie, B. J.; Rienstra, C. M. *J. Chem. Phys.* **2008**, *128*, 052207.
(8) Herbst, C.; Riedel, K.; Ihle, Y.; Leppert, J.; Ohlenschlager, O.; Gorlach, M.; Ramachandran, R. *J. Biomol. NMR* **2008**, *41*, 121−125.
(9) Kupce, E.; Kay, L. E.; Freeman, R. *J. Am. Chem. Soc.* **2010**, *132*, 18008−18011.
(10) Gopinath, T.; Veglia, G. *Angew. Chem., Int. Ed. Engl.* **2012**.
(11) Kupce, E.; Freeman, R.; John, B. K. *J. Am. Chem. Soc.* **2006**, *128*, 9606−9607.
(12) Pines, A.; Gibby, M. G.; Waugh, J. S. *J. Chem. Phys.* **1973**, *59*, 569−590.
(13) Lurie, F. M.; Slichter, C. P. *Phys. Rev. Lett.* **1963**, *10*, 403.
(14) Hartmann, S. R.; Hahn, E. L. *Phys. Rev.* **1962**, *128*, 2042.
(15) Schaefer, J.; Stejskal, E. O. *J. Am. Chem. Soc.* **1976**, *98*, 1031−1032.
(16) Levitt, M. H.; Suter, D.; Ernst, R. R. *J. Chem. Phys.* **1986**, *84*, 4243−4255.
(17) Fukuchi, M.; Ramamoorthy, A.; Takegoshi, K. *J. Magn. Reson.* **2009**, *196*, 105−109.
(18) Kolodziejski, W.; Klinowski, J. *Chem. Rev.* **2002**, *102*, 613−628.
(19) Hediger, S.; Meier, B. H.; Ernst, R. R. *Chem. Phys. Lett.* **1993**, *213*, 627−635.
(20) Hediger, S.; Meier, B. H.; Ernst, R. R. *Chem. Phys. Lett.* **1995**, *240*, 449−456.
(21) Nevzorov, A. A. *J. Magn. Reson.* **2011**, *209*, 161−166.
(22) Baldus, M.; Geurts, D. G.; Hediger, S.; Meier, B. H. *J. Magn. Reson., Ser. A* **1996**, *118*, 140−144.
(23) Baldus, M.; Petkova, A. T.; Herzfeld, J. H.; Griffin, R. G. *Mol. Phys.* **1998**, *95*, 1197−1207.
(24) Metz, G.; Wu, X. L.; Smith, S. O. *J. Magn. Reson., Ser. A* **1994**, *110*, 219−227.
(25) Schaefer, J.; McKay, R. A.; Stejskal, E. O. *J. Magn. Reson.* **1979**, *34*, 443−447.
(26) Zhang, Z.; Miao, Y.; Liu, X.; Yang, J.; Li, C.; Deng, F.; Fu, R. *J. Magn. Reson.* **2012**, *217*, 92−99.
(27) Nielsen, A. B.; Straaso, L. A.; Nieuwkoop, A. J.; Rienstra, C. M.; Bjerring, M.; Nielsen, N. C. *J. Phys. Chem. Lett.* **2010**, *1*, 1952−1956.
(28) Brinkmann, A.; Levitt, M. H. *J. Chem. Phys.* **2001**, *115*, 357−384.
(29) Lee, Y. K.; Kurur, N. D.; Helmle, M.; Johannessen, O. G.; Nielsen, N. C.; Levitt, M. H. *Chem. Phys. Lett.* **1995**, *242*, 304−309.
(30) Bjerring, M.; Nielsen, N. C. *Chem. Phys. Lett.* **2003**, *370*, 496−503.
(31) Kehlet, C.; Bjerring, M.; Sivertsen, A. C.; Kristensen, T.; Enghild, J. J.; Glaser, S. J.; Khaneja, N.; Nielsen, N. C. *J. Magn. Reson.* **2007**, *188*, 216−230.
(32) Kehlet, C. T.; Sivertsen, A. C.; Bjerring, M.; Reiss, T. O.; Khaneja, N.; Glaser, S. J.; Nielsen, N. C. *J. Am. Chem. Soc.* **2004**, *126*, 10202−10203.
(33) Gopinath, T.; Veglia, G. *J. Am. Chem. Soc.* **2009**, *131*, 5754−5756.
(34) Gopinath, T.; Verardi, R.; Traaseth, N. J.; Veglia, G. *J. Phys. Chem. B* **2010**, *114*, 5089−5095.
(35) Lazar, G. A.; Desjarlais, J. R.; Handel, T. M. *Protein Sci.* **1997**, *6*, 1167−1178.
(36) Castellani, F.; van Rossum, B.; Diehl, A.; Schubert, M.; Rehbein, K.; Oschkinat, H. *Nature* **2002**, *420*, 98−102.
(37) LeMaster, D. M.; Kushlan, D. M. *J. Am. Chem. Soc.* **1996**, *118*, 9255−9264.
(38) Igumenova, T. I.; Wand, A. J.; McDermott, A. E. *J. Am. Chem. Soc.* **2004**, *126*, 5323−5331.
(39) Franks, W. T.; Kloepper, K. D.; Wylie, B. J.; Rienstra, C. M. *J. Biomol. NMR* **2007**, *39*, 107−131.
(40) Takegoshi, K.; Nakamura, S.; Terao, T. *Chem. Phys. Lett.* **2001**, *344*, 631−637.
(41) Loening, N. M.; Bjerring, M.; Nielsen, N. C.; Oschkinat, H. *J. Magn. Reson.* **2012**, *214*, 81−90.
(42) Seidel, K.; Etzkorn, M.; Heise, H.; Becker, S.; Baldus, M. *ChemBioChem* **2005**, *6*, 1638−1647.
(43) Schubert, M.; Manolikas, T.; Rogowski, M.; Meier, B. H. *J. Biomol. NMR* **2006**, *35*, 167−173.
(44) Igumenova, T. I.; McDermott, A. E.; Zilm, K. W.; Martin, R. W.; Paulson, E. K.; Wand, A. J. *J. Am. Chem. Soc.* **2004**, *126*, 6720−6727.
(45) Hong, M.; Jakes, K. *J. Biomol. NMR* **1999**, *14*, 71−74.
(46) Lian, L. Y.; Middleton, D. A. *Prog. Nucl. Magn. Reson. Spectrosc.* **2001**, *39*, 171−190.
(47) Vuister, G. W.; Kim, S. J.; Wu, C.; Bax, A. *J. Am. Chem. Soc.* **1994**, *116*, 9206−9210.
(48) Higman, V. A.; Flinders, J.; Hiller, M.; Jehle, S.; Markovic, S.; Fiedler, S.; van Rossum, B. J.; Oschkinat, H. *J. Biomol. NMR* **2009**, *44*, 245−260.
(49) Shi, L.; Ahmed, M. A.; Zhang, W.; Whited, G.; Brown, L. S.; Ladizhansky, V. *J. Mol. Biol.* **2009**, *386*, 1078−1093.
(50) Yang, J.; Tasayco, M. L.; Polenova, T. *J. Am. Chem. Soc.* **2008**, *130*, 5798−5807.
(51) Li, S.; Su, Y.; Luo, W.; Hong, M. *J. Phys. Chem. B* **2010**, *114*, 4063−4069.
(52) Traaseth, N. J.; Veglia, G. *J. Magn. Reson.* **2011**, *211*, 18−24.
(53) Yang, J.; Parkanzky, P. D.; Bodner, M. L.; Duskin, C. A.; Weliky, D. P. *J. Magn. Reson.* **2002**, *159*, 101−110.
(54) Sperling, L. J.; Berthold, D. A.; Sasser, T. L.; Jeisy-Scott, V.; Rienstra, C. M. *J. Mol. Biol.* **2010**, *399*, 268−282.
(55) Lopez, J. J.; Kaiser, C.; Asami, S.; Glaubitz, C. *J. Am. Chem. Soc.* **2009**, *131*, 15970−15971.
(56) Wickramasinghe, N. P.; Shaibat, M.; Ishii, Y. *J. Am. Chem. Soc.* **2005**, *127*, 5796−5797.
(57) Nadaud, P. S.; Helmus, J. J.; Kall, S. L.; Jaroniec, C. P. *J. Am. Chem. Soc.* **2009**, *131*, 8108−8120.
(58) Yamamoto, K.; Xu, J.; Kawulka, K. E.; Vederas, J. C.; Ramamoorthy, A. *J. Am. Chem. Soc.* **2010**, *132*, 6929−6931.
(59) Tang, W.; Nevzorov, A. A. *J. Magn. Reson.* **2011**, *212*, 245−248.
(60) Wu, X. L.; Zhang, S. M.; Wu, X. W. *Phys. Rev. B* **1988**, *37*, 9827−9829.
(61) Agarwal, V.; Fink, U.; Schuldiner, S.; Reif, B. *Biochim. Biophys. Acta* **2007**, *1768*, 3036−3043.
(62) Ward, M. E.; Shi, L.; Lake, E.; Krishnamurthy, S.; Hutchins, H.; Brown, L. S.; Ladizhansky, V. *J. Am. Chem. Soc.* **2011**, *133*, 17434−17443.
(63) Li, Y.; Berthold, D. A.; Frericks, H. L.; Gennis, R. B.; Rienstra, C. M. *ChemBioChem* **2007**, *8*, 434−442.
(64) Shi, L.; Kawamura, I.; Jung, K. H.; Brown, L. S.; Ladizhansky, V. *Angew. Chem., Int. Ed. Engl.* **2011**, *50*, 1302−1305.
(65) Mittag, T.; Kay, L. E.; Forman-Kay, J. D. *J. Mol. Recognit.* **2010**, *23*, 105−116.
(66) Gustavsson, M.; Traaseth, N. J.; Karim, C. B.; Lockamy, E. L.; Thomas, D. D.; Veglia, G. *J. Mol. Biol.* **2011**, *408*, 755−765.
(67) Gustavsson, M.; Traaseth, N. J.; Veglia, G. *Biochim. Biophys. Acta* **2012**, *1818*, 146−153.
(68) Hong, M.; Zhang, Y.; Hu, F. *Annu. Rev. Phys. Chem.* **2011**.
(69) Su, Y.; Hong, M. *J. Phys. Chem. B* **2011**, *115*, 10758−10767.

(70) Chevelkov, V.; Faelber, K.; Schrey, A.; Rehbein, K.; Diehl, A.; Reif, B. *J. Am. Chem. Soc.* **2007**, *129*, 10195−10200.
(71) Schanda, P.; Meier, B. H.; Ernst, M. *J. Am. Chem. Soc.* **2010**, *132*, 15957−15967.
(72) Gopinath, T.; Veglia, G. *J. Magn. Reson.* **2012**, in press.
(73) Maly, T.; Debelouchina, G. T.; Bajaj, V. S.; Hu, K. N.; Joo, C. G.; Mak-Jurkauskas, M. L.; Sirigiri, J. R.; van der Wel, P. C.; Herzfeld, J.; Temkin, R. J. *J. Chem. Phys.* **2008**, *128*, 052211.
(74) Evans, J. N. S.; Appleyard, R. J.; Shuttleworth, W. A. *J. Am. Chem. Soc.* **1993**, *115*, 1588−1590.
(75) Hu, K. N.; Yau, W. M.; Tycko, R. *J. Am. Chem. Soc.* **2010**, *132*, 24−25.
(76) Comellas, G.; Lemkau, L. R.; Zhou, D. H.; George, J. M.; Rienstra, C. M. *J. Am. Chem. Soc.* **2012**, *134*, 5090−5099.